Total-Reflection X-Ray Fluorescence Spectroscopy: Analytical Signal Formation on Heterogeneous Surfaces

Kirill V. Oskolok[†],[1] Nikolai V. Alov,[1]

Axel Wittershagen,[2] Martina Mertens,[2] Bernd O. Kolbesen [2]

[1][†] Department of Analytical Chemistry, Lomonosov Moscow State University, 119899 Moscow, Russia (E-mail: oskolok@analyt.chem.msu.ru)
[2] Department of Inorganic Chemistry / Analytical Chemistry, Johann Wolfgang Goethe University of Frankfurt am Main, Marie-Curie-Str. 11, D-60439 Frankfurt am Main, Germany

The theoretical fundamentals of the analytical signal formation during the research of heterogeneous microphases on foreign substrate surfaces by total-reflection X-ray fluorescence spectroscopy were developed. The influence of the mechanism of nucleation and growth of the new phase, its morphology and sizes, the element distribution in the phase bulk on the intensity of X-ray fluorescent line of the element being determined was considered with the assumption that the substrate density is less than the phase density. The theoretical conclusions were tested during the study of the surfaces of disc glass-ceramic carbon electrodes modified by electrodeposition and co-deposition of metals from aqueous solutions under electroanalytical experiment conditions. In particular, it was found that under the constant total metal quantity on the electrode surface the change of the mechanism of metal deposition leads to the substantial change of the intensity of X-ray fluorescent line of this metal.

The main difference between total-reflection X-ray fluorescence (TXRF) analysis and the classical XRF is known being the spatial separation of primary (exciting) and secondary (fluorescent) radiation as a result of X-ray flux exposure to a sample under the grazing angles. This feature leads to a number of important advantages of TXRF: small depth of analyzed layer (~100 nm), low detection limits (10^{-9}-10^{-7} mass.%), simplicity of quantitative analysis procedure.[1] For the enumerated advantages of TXRF analysis to be attained the quality of the reflective surface should be very high and the density of reflector material – as low as possible.[1,2] Therefore TXRF is conventionally used either for the determination of very low contents of substance on a smooth quartz surface[3] or for the analysis of "light" multilayer thin-film composites (e.g., silicon wafers),[4] i.e. the analyzed surface is plane and homogeneous as a rule. For the range of analyzed subjects to be enlarged it is necessary to know the features of TXRF spectrum formation on rough surfaces. From the other hand the exploratory possibilities of TXRF are rather expansive than the analytical. In particular, the hypersensitivity to the surface roughness can be used for the study of surface morphology and the element distribution along heterogeneous surface. The aim of the present work is to study the influence of the morphology of heterogeneous surface on the intensity of the TXRF spectrum line of the element being determined.

Theoretical

TXRF is well known as a method of solid subsurface analysis based on the effect of total external reflection of primary exciting X-rays. For plane homogeneous surfaces this process can be considered as X-ray reflection from the ensemble of semitransparent monatomic layers. The X-ray fluorescence in each layer is excited by both the incident and reflected primary radiation. The less the analyzed depth and the incident angle, the less the probability of inelastic scattering of fluorescent radiation and the larger the signal to noise ratio in the TXRF spectrum. In the first approximation the dependence of the intensity of the fluorescent line of i-element ($I_{f,i}$) on its content (C_i) is

$$I_{f,i} = k\mu_{p,i}P_iI_pC_i \qquad (1)$$

where k – generalized coefficient accounting for the radiation scattering and spectrometer geometry, $\mu_{p,i}$ – mass coefficient of primary X-ray absorption, P_i – fluorescence yield, I_p – intensity of primary X-ray flux.

Analytical signal formation for a heterogeneous phase on a foreign substrate proceeds in a different way. We will consider a more frequent case – the substrate density is less than the phase density. Evidently the condition of total reflection of primary X-rays holds true for the analyzed phase. The fluorescent radiation of the phase is excited by X-rays reflected from the "phase-substrate" interface {1}, X-rays reflected from the uncovered substrate surface {2} and incident X-rays {3} (Fig. 1):

$$I_{f,i} = \sum_{j=1}^{3} I_{f,i,\{j\}} \qquad (2)$$

Hence,

$$I_{f,i,\{j\}} = \xi_{\{j\}}I_{f,i} ; \quad \xi_{\{j\}} \le 1 \qquad (3)$$

The contribution of component {1}

$$\xi_{\{1\}} \approx s_{het}(1-s_{het}) \int_{d-d_0}^{d} \exp(-\mu_{f,i}\rho l)dl \qquad (4)$$

where s_{het} – portion of substrate surface area covered by analyzed phase, $\mu_{f,i}$ – mass coefficient of fluorescence

attenuation, ρ – phase density, d – thickness of phase layer, d_0 – analyzed depth of phase. It should be pointed out that there are certain optimal values of the degree of substrate surface filling by phase (s_{opt}) and the thickness of phase layer (does not exceed d_0), under which $\xi_{\{1\}}$ value is maximum. Indeed,

$$\partial\xi_{\{1\}}/\partial s_{het} = 0 \qquad \text{if } 0 < s_{opt} < 1$$
$$\xi_{\{1\}} \sim \left(1 - \exp(-\mu_{f,i}\rho d)\right) \quad \text{if } d \le d_0 \qquad (5)$$
$$\xi_{\{1\}} \sim \exp(-\mu_{f,i}\rho d) \qquad \text{if } d > d_0$$

These optimal values depend on the nature of the phase and the energy of the primary and fluorescent radiation. If the phase layer thickness exceeds an optimal value, the signal to noise ratio in the TXRF spectrum is reduced as a result of absorption and inelastic scattering of the fluorescent radiation in the phase bulk. Under the small thickness of the phase layer ($d \le d_0$) and low degree of surface filling ($s_{het} \ge 0$) the formula (4) is simplified

$$\xi_{\{1\}} \approx s_{het} \int_{d-d_0}^{d} \exp(-\mu_{f,i}\rho l)dl \qquad (6)$$

Under the considerable thickness of the phase layer ($d > d_0$) and high degree of substrate surface filling ($s_{het} \to 1$)

$$\xi_{\{1\}} \to 0 \qquad (7)$$

In the first approximation the contribution of component {2} is

$$\xi_{\{2\}} \sim l_{het}(1 - s_{het})d \qquad (8)$$

where l_{het} – perimeter of zone covered by phase. $\xi_{\{2\}}$ value is perceptible in the case of the considerable thickness of phase layer and degree of surface filling. However factor {2} promotes not so increasing the intensity of characteristic line as the primary X-ray scattering and signal to noise ratio reducing. Hence the contribution of component {2} can be neglected.

The phase morphology can be conveniently described by the complicated function ($f_{\{3\}}$) of area mean radius of curvature of the phase surface ($\overline{R_{av}}$). The contribution of component {3} is

$$\xi_{\{3\}} \approx f_{\{3\}}\left(\overline{R_{av}}\right)\cdot s_{het} \int_{0}^{d} \exp(-\mu_{f,i}\rho l)dl =$$
$$= \frac{f_{\{3\}}\left(\overline{R_{av}}\right)\cdot s_{het}}{\mu_{f,i}\rho}\left(1 - \exp(-\mu_{f,i}\rho d)\right) \qquad (9)$$
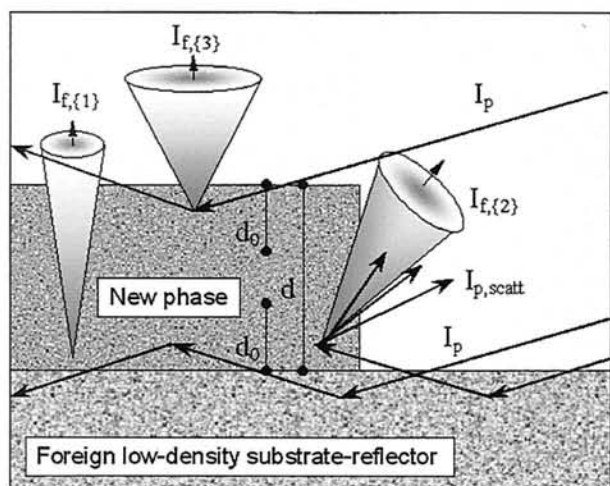

Fig. 1. The scheme of excitation of TXRF spectrum of the heterogeneous phase on the foreign substrate-reflector (the density of the reflector is less than the density of the phase).
The physical meaning of the function $f_{\{3\}}$ is the portion of quasi-plane areas on the phase surface. If this parameter value is low

then the efficiency of primary X-ray scattering is increased and the signal to noise ratio in the TXRF spectrum is reduced. Moreover the variation of the incident angle to the spherical surface does not practically change signal to noise ratio. Thus

$$\left.\begin{array}{l} f_{\{3\}} \to 1 \quad \text{if } \overline{R_{av}} \gg d \\ f_{\{3\}} \to 0 \quad \text{if } \overline{R_{av}} \approx d \end{array}\right\} \qquad (10)$$

Since the features of heterogeneous surface morphology are due to the *mechanisms of nucleation and growth of the phase*, we will consider the influence of main types of them on the analytical signal formation in TXRF-spectra.

Frank-van der Merwe mechanism.
It is a mechanism of layer-by-layer 2D-growth.[5] The uniform film of the phase covers the substrate surface ($f_{\{3\}}=1$). **Slight scattering** of primary X-rays takes place. In the case of the thin film formation ($d < d_0$):

$$I_{f,i} \sim \frac{S_{het}}{\mu_{f,i}\rho}\left(1 - \exp(-\mu_{f,i}\rho d)\right) \qquad (11)$$

In the case of the thick film formation ($d \ge d_0$ or $d \gg d_0$):

$$I_{f,i} \sim \frac{S_{het}}{\mu_{f,i}\rho} \qquad (12)$$

Thus during the growth of the phase film an intensity of X-ray fluorescent line is increased and finally reaches maximum value.

Volmer-Weber mechanism.
It is a mechanism of 3D-island growth.[5] As a rule the most part of the substrate surface is uncovered by the phase. In the case of prevailing lateral growth of 3D-nuclei: $0 < f_{\{3\}} < 1$. **Moderate scattering** of primary X-rays takes place. In the case of the formation of the small 3D-islands ($\overline{R_{av}} \gg d$; $d < d_0$):

$$I_{f,i} \sim \frac{S_{het}}{\mu_{f,i}\rho}\left(1 + f_{\{3\}}\left(\overline{R_{av}}\right)\right)\cdot\left(1 - \exp(-\mu_{f,i}\rho d)\right) \qquad (13)$$

In the case of the formation of the large 3D-islands ($\overline{R_{av}} \gg d$; $d \ge d_0$):

$$I_{f,i} \sim \frac{S_{het}}{\mu_{f,i}\rho}\cdot f\left(\overline{R_{av}}\right)+$$
$$+ \frac{S_{het}}{\mu_{f,i}\rho}\exp(-\mu_{f,i}\rho d)\cdot\left(\exp(\mu_{f,i}\rho d_0) - f_{\{3\}}\left(\overline{R_{av}}\right) - 1\right) \qquad (14)$$

In the case of the formation of the very large 3D-crystallites ($\overline{R_{av}} \gg d$; $d \gg d_0$):

$$I_{f,i} \sim \frac{f_{\{3\}}\left(\overline{R_{av}}\right)\cdot s_{het}}{\mu_{f,i}\rho} \qquad (15)$$

Thus the ultimate intensity of the fluorescent line is finite and less than under thin film formation. It amounts the maximum value under the increase of lateral growth rate of nuclei.

In the case of balanced (vertical and lateral) growth of 3D-nuclei: $f_{\{3\}} \to 0$. **Intense scattering** of primary X-rays takes place. In the case of the formation of the small 3D-islands ($\overline{R_{av}} \approx d$; $d < d_0$):

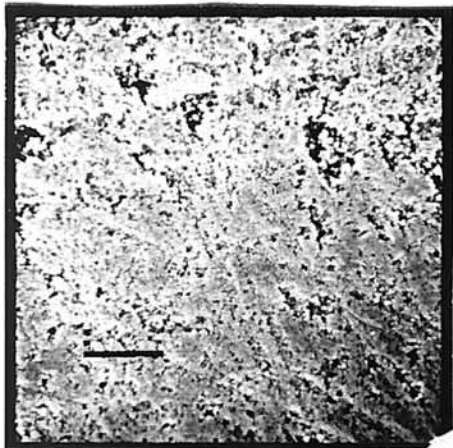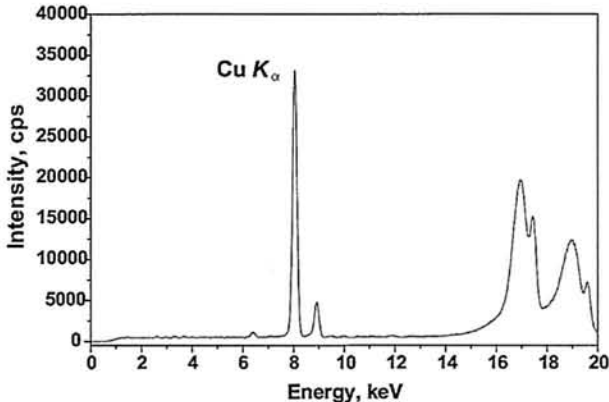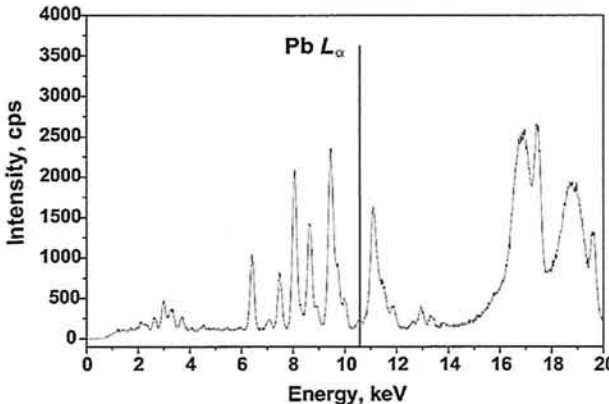$$I_{f,i} \sim \frac{S_{het}}{\mu_{f,i}\rho}\left(1 - \exp(-\mu_{f,i}\rho d)\right) \qquad (16)$$
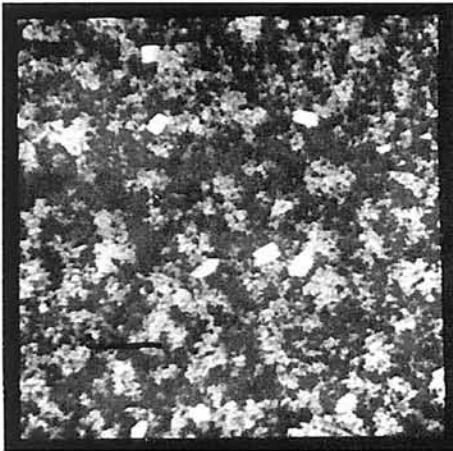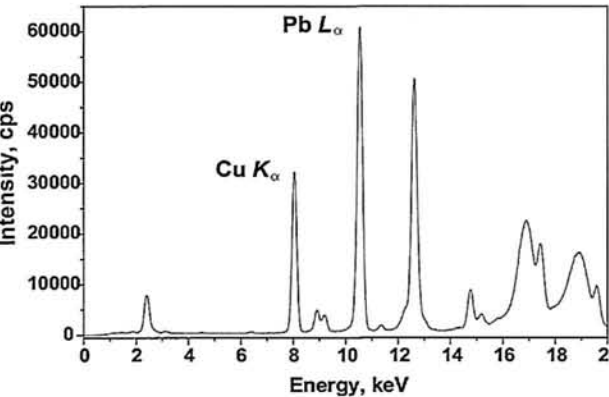
Metal and alloy electrodeposit on GCC electrode surface	
SEM images	TXRF spectra

Cu thin film (a)

Magnification ×200

Pb 3D-crystallites (b)

Magnification ×4000

Pb 3D-crystallites + thin film of Cu-Pb solid solution (c)

Magnification ×2000

Fig. 2. The influence of the electrodeposit morphology and the distribution of the metal content in the electrodeposit bulk on the intensity of the X-ray fluorescent lines of the metals (analytical signals) in the TXRF spectra of the electrochemically modified surfaces of the GCC electrodes; the total quantities of deposited metals are comparable (see clarification in the text).

In the case of the formation of the large 3D-islands ($\overline{R_{av}} \approx d$; $d \geq d_0$):

$$I_{f,i} \sim \frac{S_{het}}{\mu_{f,i}\rho}\left(\exp\left(\mu_{f,i}\rho d_0\right)-1\right)\exp\left(-\mu_{f,i}\rho d\right) \qquad (17)$$

In the case of the formation of the very large 3D-crystallites ($\overline{R_{av}} \approx d$; $d \gg d_0$):

$$I_{f,i} \rightarrow 0 \qquad (18)$$

Thus the fluorescent line intensity is increased on early stages of the phase formation only. On late stages it is decreased and the ultimate intensity of the fluorescent line is very low and indefinite. In this case the spatial separation of exciting and fluorescent radiation – the main TXRF advantage – does not practically proceed. Hence the fluorescent line intensity is on the noise level in TXRF-spectrum due to the following reasons. Firstly the total phase content on the substrate-reflector is very low. Secondly the primary X-ray flux in TXRF is much less than in classic XRF.

Stranski-Krastanov mechanism.

It is a mechanism of monolayer(s) + 3D-island growth.[5] The fluorescent line intensity is comparable with the intensity in the case of the mechanism of layer-by-layer 2D-growth. However the signal to noise ratio in TXRF-spectrum is significantly less.

Experimental

For the approval of our theoretical conclusions we have studied the metal and alloy electrodeposits on the plane surfaces of solid electrodes manufactured from the foreign low-density material. The samples were prepared by the electrochemical deposition and co-deposition of metals from $n \cdot 10^{-4}$M (Cu, Pb)(NO$_3$)$_2$ + 0.01M HNO$_3$ solutions on the surfaces of disc glass-ceramic carbon (GCC) electrodes (radius 3 mm) during solution mixing. GCC is an advanced type of glassy carbon with excellent mechanical and electrochemical properties for the electrode preparation for anodic stripping voltammetry.[6] The surfaces of disc GCC electrodes were mechanically and electrochemically polished before the metal electrodeposition. The electrolysis potential was -1000 mV (SCE). The electrolysis time was 300 s. The metal electrodeposition technique was described in detail elsewhere.[7] The morphology of origin and electrochemically modified surfaces of the GCC electrodes was studied by scanning electron microscopy (SEM) with use of electron-probe microanalyzer CAMEBAX-microbeam. TXRF measurements were performed with an ATOMIKA EXTRA II A spectrometer using MoK$_\alpha$ (17.5 keV) primary excitation.[8]

Results and discussion

The results of TXRF-spectrum interpretation are in a good agreement with the information about mechanisms of metal and alloy electrodeposition. These mechanisms were earlier studied in detail with use of a number of methods of solid surface analysis.[7, 9, 10] The late stages of copper electrodeposition on GCC electrode surface proceed by Frank-van der Merwe mechanism. Copper forms a thin film (thickness ~1 μm) covering the entire electrode surface. Lead electrodeposition proceeds by classic Volmer-Weber mechanism. Lead forms numerous 3D-crystallites with sizes up to 5-8 μm. In the case of the electrochemical co-deposition of these metals, the considerable part of the lead goes into the copper thin film and a

solid solution is formed. In the case of copper deposition and co-deposition with lead, the CuK$_\alpha$ intensity is high and constant (compare Fig. 2a, 2c). In the case of lead deposition, the PbL$_\alpha$ intensity is on the noise level in the TXRF-spectrum in spite of the quantities of copper and lead electrodeposits are comparable (Fig. 2a, 2b). In the case of electrochemical co-deposition of the metals, the PbL$_\alpha$ intensity is increased by more than 600 times (compare Fig. 2b, 2c). The multiple fluorescent lines near the pointer of PbL$_\alpha$ line in the TXRF-spectrum belong to some trace elements (Ag, Pt, etc.) localizing on the plane areas of the GCC electrode surface uncovered by the lead phase (Fig. 2b). Silver is a component of the reference electrode (SCE). Platinum is a material of the counter electrode of the used electrochemical cell. Although the total quantities of these impurities on the surface of the GCC electrode is less than the lead quantity by 10^2-10^3 times at least, the intensities of their fluorescent lines is significantly greater than the intensity of the PbL$_\alpha$ line! Other examples proving our theoretical conclusions are considered in detail elsewhere.[8]

Conclusions

Thus the fundamentals of an analytical signal formation during TXRF analysis of heterogeneous surfaces were developed. The influence of analyzed surface morphology on the intensity of TXRF-spectrum line was considered. It was shown that TXRF can be effectively applied for the identification of mechanisms of nucleation and growth of metal and alloy electrodeposits on foreign low-density substrates. The results of the present work proves the necessity of the account of the influence of the macroscopic properties of the analyzed heterogeneous surface on the intensity of X-ray fluorescent line of the element being determined during the quantitative TXRF analysis (under the usage of the "standardless" method of fundamental physical parameters especially).

References

1. R. Klockenkämper, *"Total-Reflection X-ray Fluorescence Analysis"*, **1997**, Wiley, NY.
2. L. Moens, W. Devos, R. Klockenkämper, and A. von Bohlen, *Trends in Analytical Chemistry*, **1994**, *13*, 198.
3. M. Mertens, C. Rittmeyer, P. Rostam-Khani, and B.O. Kolbesen, in *CANAS '97, Colloq. Anal. Atomspektrosk.*, Universität Leipzig und UFZ Leipzig-Halle, Germany, **1998**, 441.
4. P. Wobrauschek, P. Kregsamer, R. Goergl, and C. Streli, in *Proceedings of the European Conf. Energy Dispersive X-ray Spectrom.*, Lisboa, Portugal, June 23-29, **1996**.
5. W.J. Lorenz, and G. Staikov, *Surf. Sci.*, **1995**, 335, 32.
6. I.P. Viter, A.I. Kamenev, A.A. Sidakov, and V.N. Zygan, *Zhurnal analiticheskoi khimii*, **1994**, *49*, 1295.
7. N.V. Alov, K.B. Kalmykov, A.I. Kamenev, K.A. Kovalskii, K.V. Oskolok, and V.K. Runov, *Surf. Investigation*, **1999**, *14*, 775.
8. N.V. Alov, K.V. Oskolok, A. Wittershagen, M. Mertens, C. Rittmeyer, and B.O. Kolbesen, in *Abstracts of the 8th Conf. Total Reflection X-ray Fluorescence Anal. Related Methods (TXRF-2000)*, Vienna, Austria, September 25-29, **2000**, 65.
9. N.V. Alov, K.B. Kalmykov, A.I. Kamenev, and K.V. Oskolok, in *Abstracts of the 15th Int. Congr. X-ray Optics Microanal. (ICXOM XV)*, Antwerp, Belgium, August 24-27, **1998**, 49.
10. N.V. Alov, and K.V. Oskolok, *J. Anal. At. Spectrom.*, **1999**, *14*, 425.